INSTITUTE OF PHYSICS PUBLISHING SEMICONDUCTOR SCIENCE AND TECHNOLOGY
Semicond. Sci. Technol. **17** (2002) L59–L62 PII: S0268-1242(02)39380-5

LETTER TO THE EDITOR

Electron initiated impact ionization in AlGaN alloys

C Bulutay

Department of Physics, Bilkent University, Ankara, 06533, Turkey

Received 11 July 2002, in final form 22 August 2002
Published 19 September 2002
Online at stacks.iop.org/SST/17/L59

Abstract
Detailed impact ionization (II) analysis of electrons is presented for AlGaN alloys as a vital resource for solar-blind avalanche photodiode and high power transistor applications. Necessary ingredients for the II characterization are supplied from a recent experiment on the GaN end, and a Keldysh analysis for the AlN end, of the alloy AlGaN. High-field electron dynamics are simulated using an ensemble Monte Carlo framework, accounting for all valleys in the lowest two conduction bands, obtained from accurate empirical pseudopotential band structure computations. The effect of alloy scattering on II is considered and observed to be significant. For any $Al_xGa_{1-x}N$ alloy, the electron II coefficients are found to obey the form, $A\exp(-K/F)$, for the electric field, F.

The $Al_xGa_{1-x}N$ alloy is emerging as a complementary material system for high power electronic and optoelectronic applications. Specifically, $GaN/Al_xGa_{1-x}N$ heterojunction bipolar transistors and $Al_xGa_{1-x}N$ avalanche photodiodes (especially for solar-blind purposes) are two important devices to benefit from this material system. For both these devices, operating at high fields, it is compulsory to understand the impact ionization (II) process. However, there has been no experimental work on II for the $Al_xGa_{1-x}N$ system. As a matter of fact, measurement of the II coefficient is rather a formidable task, which requires maintaining uniform fields and avoiding instabilities [1]. To meet this demand from the computational side, in this letter we provide results for the characterization of electron initiated II in $Al_xGa_{1-x}N$ for a wide range of alloy compositions.

We utilize our accurate band structures for GaN and AlN [2, 3] based on the empirical pseudopotential technique fitted to available experimental results and first-principles computations, with special emphasis given to conduction band properties. For the band structure of the alloy, $Al_xGa_{1-x}N$, we resort to linear interpolation (Vegard's law) between the pseudopotential form factors of the constituent binaries as, for instance, in the work of Goano *et al* [4] Our approach for high-field transport relies on the ensemble Monte Carlo (EMC) technique [5], including all major scattering processes: acoustic, non-polar and polar optical phonons, ionized impurity, alloy and II scatterings. We consider the initial free carrier density to be low, so that the carrier–carrier scattering can be neglected; of course, after the initiation of an II breakdown, there may be a large carrier density where this scattering mechanism becomes significant.

Prior to EMC simulation, we perform a band edge analysis throughout the computed bands of $Al_xGa_{1-x}N$, and extract the band edge energy, effective mass and non-parabolicity parameters of all valleys in the lowest two conduction bands, which are located at Γ_1, U, K, M and Γ_3 points. To account for the remaining excited bands, we further append an additional higher-lying parabolic free electron band. Table 1 lists these parameters for the alloy mole fractions used in this work. In lieu of this band pre-processing, we can now proceed to use the computationally appealing analytical-band variant of the EMC technique. It may be noted that more sophisticated full band EMC approaches exist, as applied to GaN [6, 7]. Despite the poor representation of the band structure at higher energies for a model like ours, it has been tested to reproduce the experimental as well as full band results in the same context of II in bulk and p–i–n diodes [8, 9]. Furthermore, the computational overhead of a full band EMC simulation should also be kept in mind. As a matter of fact, II is a rare event among all electrons, and requires accurate representation of carriers in the high-energy tail of the distribution function. Thus, we employ 25 000 electrons in the ensemble, with a time step of less than 0.1 fs, and a total simulation time of about 1 ps.

Table 1. Band edge analysis throughout the lowest two conduction bands of $Al_xGa_{1-x}N$ alloys; E is the band edge energy, m^* is the density of states effective mass and α is the non-parabolicity factor (other than the lowest valley, two-band $\vec{k}\cdot\vec{p}$ values are preferred). Equivalent valley multiplicities N_v are also included. Note that the ordering of the U and K valleys is interchanged at an aluminium mole fraction of 0.6.

E (eV) m^*/m_0 α (eV^{-1})	GaN	$Al_{0.2}Ga_{0.8}N$	$Al_{0.4}Ga_{0.6}N$	$Al_{0.6}Ga_{0.4}N$	$Al_{0.8}Ga_{0.2}N$	AlN
Γ_1 ($N_v = 1$)	0	0	0	0	0	0
	0.2	0.214	0.227	0.238	0.246	0.26
	0.262	0.243	0.230	0.221	0.213	0.207
U ($N_v = 6$)	1.34	1.285	1.233	1.181	1.131	1.05
	0.442	0.456	0.468	0.486	0.487	0.495
	0.064	0.056	0.049	0.043	0.039	0.035
K ($N_v = 2$)	1.59	1.444	1.307	1.179	1.057	0.9
	0.47	0.477	0.483	0.478	0.488	0.488
	0.055	0.050	0.045	0.042	0.039	0.106
M ($N_v = 3$)	1.87	1.830	1.798	1.769	1.741	1.68
	0.565	0.577	0.590	0.604	0.617	0.629
	0.035	0.030	0.026	0.023	0.020	0.017
Γ_3 ($N_v = 1$)	2.14	2.23	2.312	2.390	2.462	2.49
	0.439	0.463	0.485	0.507	0.529	0.55
	0.056	0.046	0.039	0.032	0.027	0.023
Free electron	3.5	3.6	3.7	3.8	3.9	4
band ($N_v = 1$)	1	1	1	1	1	1
	0	0	0	0	0	0

Table 2. A and K values in the electron II coefficient expression, $A\exp(-K/F)$, where F is the electric field. A temperature of 300 K and an ionized impurity concentration of 10^{17} cm^{-3} are used.

	GaN	$Al_{0.2}Ga_{0.8}N$	$Al_{0.4}Ga_{0.6}N$	$Al_{0.6}Ga_{0.4}N$	$Al_{0.8}Ga_{0.2}N$	AlN
A (cm^{-1})	1.1438×10^7	1.5126×10^7	2.0647×10^7	1.7974×10^7	1.2993×10^7	8.8750×10^6
K (MV cm^{-1})	23.8933	31.6707	36.6251	37.7751	36.3373	37.5904

With this parameter set, we can resolve fast processes while assuring steady-state operation for all fields considered.

The only available experimental report about II relevant to our work is that on GaN by Kunihiro *et al* [10]. Using our EMC framework, we are able to fit to their electron ionization coefficient with an II scattering rate of $P_{\mathrm{II}}^{\mathrm{GaN}}(1/\mathrm{s}) = 2.5 \times 10^6 \left(E_{\mathrm{in}} - E_{\mathrm{th}}^{\mathrm{GaN}}\right)^8 u(E_{\mathrm{in}} - E_{\mathrm{th}}^{\mathrm{GaN}})$, where E_{in} is the energy of the electron in electronvolts, $E_{\mathrm{th}}^{\mathrm{GaN}} = 4$ eV is the II threshold energy, and $u(\cdot)$ is the unit step function. This expression, when compared to the *ab initio* results for GaN [11], possesses similar exponent and threshold values, but a reduced coefficient. On the other hand, for $Al_xGa_{1-x}N$ Ando *et al* [7] have used linear interpolation between the II rates of GaN and AlN, assuming for simplicity a null value for AlN. Aiming for a more realistic estimation for AlN, we make use of the Keldysh approach, which is valid for parabolic bands, while Bloch overlaps are taken into account via the *f*-sum rule [12]. The corresponding II scattering rate comes out as $P_{\mathrm{II}}^{\mathrm{AlN}}(1/\mathrm{s}) = 7.04 \times 10^{11}\left(E_{\mathrm{in}} - E_{\mathrm{th}}^{\mathrm{AlN}}\right)^2 u\left(E_{\mathrm{in}} - E_{\mathrm{th}}^{\mathrm{AlN}}\right)$, where $E_{\mathrm{th}}^{\mathrm{AlN}} = 6.84$ eV. Examining the forms of these two scattering rate expressions, we see that GaN possesses a soft threshold, whereas the Keldysh treatment demands a hard threshold for AlN. The latter should not be undermined as well; as Hess pointed out, the Keldysh approach can still adequately represent the experimental data for the case of steady-state phenomena [1].

During the EMC simulation we keep a fixed carrier population, and after an II event we discard the generated electron–hole pair. However, for the purposes of this work we are more sensitive to the energy loss of the impacting electron and we avoid the simplistic treatment of restarting this electron from the conduction band minimum, as is usually done [7, 13]. Utilizing the results of first-principles characterization on II by Jung *et al* [14], we employ a piecewise linear functional relation between the initial (E_{in}) and final (E_{fin}) energies of the impacting electron, measured from the conduction band minimum, as

$$E_{\mathrm{fin}} = \begin{cases} 0, & E_{\mathrm{in}} < E_{\mathrm{th}}^{AB} \\ c_1\left(E_{\mathrm{in}} - E_{\mathrm{th}}^{AB}\right), & E_{\mathrm{th}}^{AB} \leqslant E_{\mathrm{in}} \leqslant E_{\mathrm{br}}^{AB} \\ c_2\left(E_{\mathrm{in}} - E_0^{AB}\right), & E_{\mathrm{br}} < E_{\mathrm{in}}, \end{cases}$$

where $E_{\mathrm{br}}^{AB} = c_3 E_{\mathrm{gap}}^{AB}$, $E_0^{AB} = \left[c_1 E_{\mathrm{th}}^{AB} + (c_2 - c_1)E_{\mathrm{br}}^{AB}\right]/c_2$, and E_{th}^{AB} is the alloy II threshold energy obtained using Vegard's law from the binaries E_{th}^{A} and E_{th}^{B}. The energy coefficients above, c_1, c_2 and c_3, are practically taken to be material independent [15], and we use the values of Jung *et al*, $c_1 = 0.55$, $c_2 = 0.267$, $c_3 = 2.11$, extracted from GaAs data at 300 K [14]. Incorporating the first-principles II scattering rate expression of this reference to our EMC formalism yields excellent agreement with the experimental results for GaAs [10], making us confident about the validity of this approach.

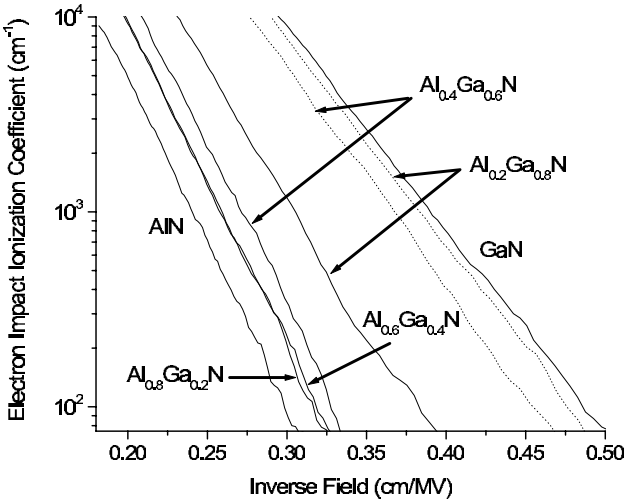

Figure 1. Electron II coefficient versus inverse electric field. Dotted curves indicate the results when alloy scattering is not included. The curves for $Al_{0.6}Ga_{0.4}N$ and $Al_{0.8}Ga_{0.2}N$ merge at higher fields. These results are obtained for a temperature of 300 K and an ionized impurity concentration of 10^{17} cm^{-3}.

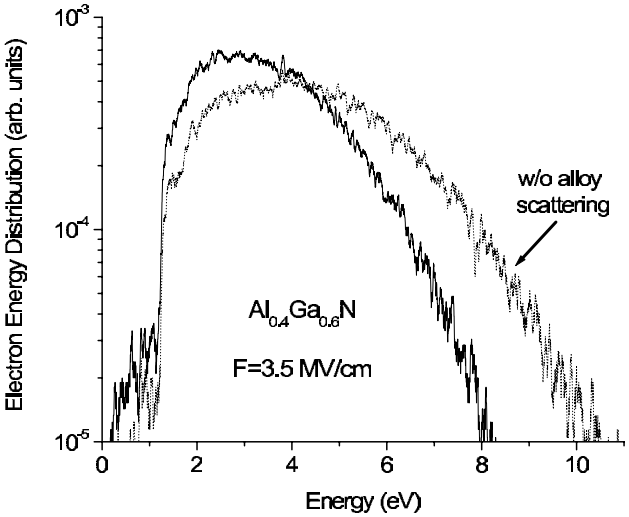

Figure 2. Electron energy distribution for $Al_{0.4}Ga_{0.6}N$ at an electric field of 3.5 MV cm^{-1}, with (solid curve) and without (dotted curve) alloy scattering. A temperature of 300 K and an ionized impurity concentration of 10^{17} cm^{-3} are considered.

Returning to the $Al_xGa_{1-x}N$ system, the electron II coefficient, α, for several alloy compositions are plotted in figure 1 with respect to the electric field, F. These results are obtained for a temperature of 300 K and an ionized impurity concentration of 10^{17} cm^{-3}. We note that these curves do not obey Wolff's form, $A\exp(-K/F^2)$, but rather can be faithfully represented using Shockley's form of $A\exp(-K/F)$; refer to table 2 for a list of these constants, A and K. In this regard, we find it useful to add the remark of Bude and Hess [16] that the functional dependence of α on F is closely related to the rise of the density of states in the most important energy range, and not as much to the question of whether lucky electrons are important for ionization or not.

In a semiconductor alloy, the scattering of free carriers due to deviations from the virtual crystal model, as also employed in this work, has been termed alloy scattering [12]. Recently, Farahmand and Brennan [17] have addressed alloy scattering in group-III nitride ternary alloys, using the conduction band offset between the binaries as the alloy potential. They have argued that this approach yields an upper bound for alloy scattering. As a representative value, in our work we use $U_{\text{alloy}} = 0.91$ eV, which is half the corresponding GaN/AlN conduction band offset. The dotted curves in figure 1, corresponding to aluminium mole fractions of 0.2 and 0.4, indicate that when alloy scattering is turned off II is significantly enhanced. In contrast, the elastic nature of the alloy scattering might initially suggest a marginal effect on the electron energy distribution. However, the deviation of the electron wave vector away from the electric field due to elastic scattering causes deceleration in the drift cycles, hence a loss in the energy of such an electron, lowering its potential for II. Figure 2 illustrates this point for $Al_{0.4}Ga_{0.6}N$ (which is an important alloy composition for solar-blind applications) at an electric field value of 3.5 MV cm^{-1}; the depletion of the high-energy tail of the distribution function due to alloy scattering explains the decrease in the II coefficient obtained in figure 1. However, we would like to draw attention to two simplifications in our approach inherited from the treatment of Fischetti and Laux [18]. The alloy scattering is implemented as an intra-valley process due to its small wavelength attenuation [18]; in the case of closely located valleys, such as U and M, this may become rather crude. More importantly, the distribution of the final scattering angles is assumed to be isotropic, even though at higher energies alloy scattering attains a forward directional character [19]. Thus, we are led to think that the effect of the alloy scattering may still be somewhat overestimated.

In summary, we present results for the electron II coefficient of AlGaN alloys and we offer closed form expressions for its functional dependence for a wide range of alloy compositions. A detailed discussion of the role of alloy scattering in this context is also included. We hope that this work will initiate further experimental and theoretical studies.

Acknowledgments

The author would like to express his gratitude to Professor K Tomizawa. This work is supported by the Scientific and Technical Research Council of Turkey (TÜBİTAK).

References

[1] Balkan N, Ridley B K and Vickers A J (ed) 1993 *Negative Differential Resistance and Instabilities in 2-D Semiconductors* (New York: Plenum)
[2] Bulutay C, Ridley B K and Zakhleniuk N A 2000 *Phys. Rev.* B **62** 15754
[3] Bulutay C, Ridley B K and Zakhleniuk N A 2002 *Physica* B **314** 63
[4] Goano M, Bellotti M E, Ghillino E, Garetto C, Ghione G and Brennan K F 2000 *J. Appl. Phys.* **88** 6476
[5] Tomizawa K 1993 *Numerical Simulation of Submicron Semiconductor Devices* (Norwood: Artech)
[6] Kolník J, Oğuzman İ H, Brennan K F, Wang R and Ruden P P 1997 *J. Appl. Phys.* **81** 726
[7] Ando Y *et al* 2000 *IEEE Trans. Electron Devices* **47** 1965
[8] Dunn G M, Rees G J, David J P R, Plimmer S A and Herbert D C 1997 *Semicond. Sci. Technol.* **12** 111

[9] Dunn G M, Ghin R, Rees G J, David J P R, Plimmer S and Herbert D C 1999 *Semicond. Sci. Technol.* **14** 994
[10] Kunihiro K, Kasahara K, Takahashi Y and Ohno Y 1999 *IEEE Electron Device Lett.* **20** 608
[11] Reigrotzki M, Dür M, Schattke W, Fitzer N, Redmer R and Goodnick S M 1997 *Phys. Status Solidi* b **204** 528
[12] Ferry D K 2000 *Semiconductor Transport* (London: Taylor and Francis)
[13] Farahmand M and Brennan K F 1999 *IEEE Trans. Electron Devices* **46** 1319
[14] Jung H K, Nakano H and Taniguchi T 1999 *Physica* B **272** 244
[15] Mouton O, Thobel J L and Fauquembergue R 1997 *J. Appl. Phys.* **81** 3160
[16] Bude J and Hess K 1992 *J. Appl. Phys.* **72** 3554
[17] Farahmand M, Garetto C, Bellotti E, Brennan K F, Goano M, Ghillino E, Ghione G, Albrecht J D and Ruden P P 2001 *IEEE Trans. Electron Devices* **48** 535
[18] Fischetti M V and Laux S E 1996 *J. Appl. Phys.* **80** 2234
[19] Yeom K, Hinckley J M and Singh J 1996 *J. Appl. Phys.* **80** 6773